Supporting information of publication: On the relation of structure and dynamics in aromatic ring-tail structured liquids

Rolf Zeißler,[1] Jan Philipp Gabriel,[2] Dorthe Posselt,[3] and Thomas Blochowicz[1]

[1] *Institute for Condensed Matter Physics, Technical University of Darmstadt, Germany*
[2] *Institute of Materials Physics in Space, German Aerospace Center, 55170 Cologne, Germany*
[3] *IMFUFA, Centre for Frustrated Molecular Interactions, Dept. of Science and Environment, Roskilde University, Denmark*

This supporting information serves to provide additional information about the fit model used to describe the X-ray scattering curves and to compare it with small-angle scattering models used for the prepeak and the plateau region instead of the Gaussian peak and Ornstein-Zernike model. The model finally used is a superposition of different model functions, yielding peak positions and widths without making assumptions about the exact physical mechanism underlying the structure formation in the liquid. The main scattering peak and the intramolecular peak at $\approx 3\,\text{Å}^{-1}$ are described by Lorentzian functions $I_{\text{Li}}(q) = A_{\text{Li}} \cdot \frac{w_{\text{Li}}}{\pi((q-q_{\text{Li,peak}})^2+w_{\text{Li}}^2)}$ with amplitude A_{Li}, half width at half maximum w_{Li} and peak position $q_{\text{Li,peak}}$. The index i=1 represents the main scattering peak and the index i=2 the intramolecular peak which is fixed for a given system (no temperature dependence). The prepeak is described by a Gaussian peak function $I_{\text{G}}(q) = A_{\text{G}} \cdot \frac{\sqrt{\ln(2)/\pi}}{w_{\text{G}}} \cdot \exp(-((q-q_{\text{G,peak}})/w_{\text{G}})^2 \cdot \ln(2))$ with amplitude A_{G}, half width at half maximum w_{G} and peak position $q_{\text{G,peak}}$. The plateau contribution at low q is described by an Ornstein-Zernike function $I_{\text{OZ}}(q) = \frac{A_{\text{OZ}}}{1+(q\xi_{\text{OZ}})^2}$ with the correlation length ξ_{OZ} and amplitude A_{OZ}. The total fit function reads as follows:

$$\begin{aligned} I(q) = {} & \frac{A_{\text{OZ}}}{1+(q\xi_{\text{OZ}})^2} \\ & + A_{\text{G}} \cdot \frac{\sqrt{\ln(2)/\pi}}{w_{\text{G}}} \cdot \exp(-((q-q_{\text{G,peak}})/w_{\text{G}})^2 \cdot \ln(2)) \\ & + A_{\text{L1}} \cdot \frac{w_{\text{L1}}}{\pi((q-q_{\text{L1,peak}})^2+w_{\text{L1}}^2)} \\ & + A_{\text{L2}} \cdot \frac{w_{\text{L2}}}{\pi((q-q_{\text{L2,peak}})^2+w_{\text{L2}}^2)}. \end{aligned} \tag{1}$$

Tbl. II shows the parameters obtained with this fitting approach for the different phenylalkanes at the different temperatures investigated.

In the following, we will give a short explanation of why this model function was chosen. A Lorentzian function was chosen to model the main scattering peak since it is the dominant contribution to the scattering curves and its shape is least obstructed by the other contributions. Evaluation of the data revealed that there is no need to introduce asymmetry or mixing of Gaussian and Lorentzian models to describe this peak for none of the liquids over their respective temperature ranges. In a similar fashion the intramolecular peak was modeled by a Lorentzian since the scattering curves at room temperature provide no incentive to select a different model function. Regarding the prepeak the choice was made according to literature. Instead of a constant background we opted for an Ornstein-Zernike function to account for the plateau at low q since adding a constant background turned out to be insufficient to describe all the scattering curves. This choice also makes sense regarding the physical origin of the low q plateau. In one component liquids, that have no heterogeneities on large length scales, the static structure factor for $q \to 0$, $S_0(T)$, reads:

$$S_0(T) = \rho k_{\text{B}} T \kappa_{\text{T}}(T), \tag{2}$$

as a consequence of density fluctuations. Here ρ is the mean number density of molecules and $\kappa_T(T)$ the isothermal compressibility, while k_{B} is the Boltzmann factor [1]. It is therefore reasonable to assume that the low q plateau in the scattering curves obtained in this work also originates from density fluctuations which should not contribute at arbitrarily large values of q but rather decay with a characteristic length scale.

Fig. 1 shows the position of the main scattering peak of the 1-phenylalkanes in dependence on temperature. The peak positions are similar at a given temperature and shift to higher q values with increasing temperature. This is to be expected since density increases with decreasing temperature and average intermolecular distances therefore decrease.

Fig. 2 a) shows the amplitude A_{OZ} of the Ornstein-Zernike function used to describe the plateau region at low q. For P19, A_{OZ} increases with increasing temperature and follows to good approximation a power law $A_{\text{OZ}} \propto T^{2.5}$ (black

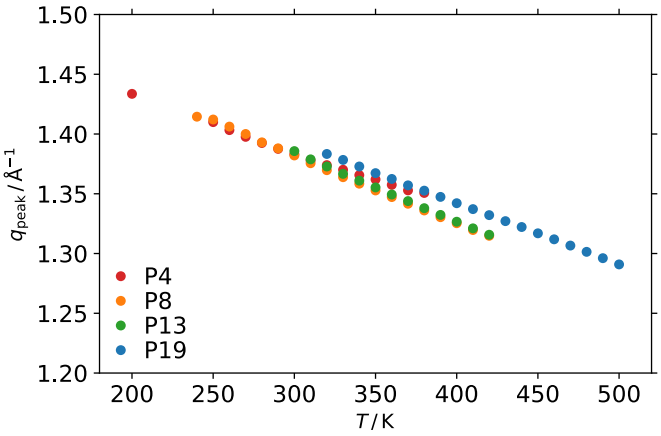

FIG. 1: Position of the main scattering peak of the 1-phenylalkanes in dependence on temperature.

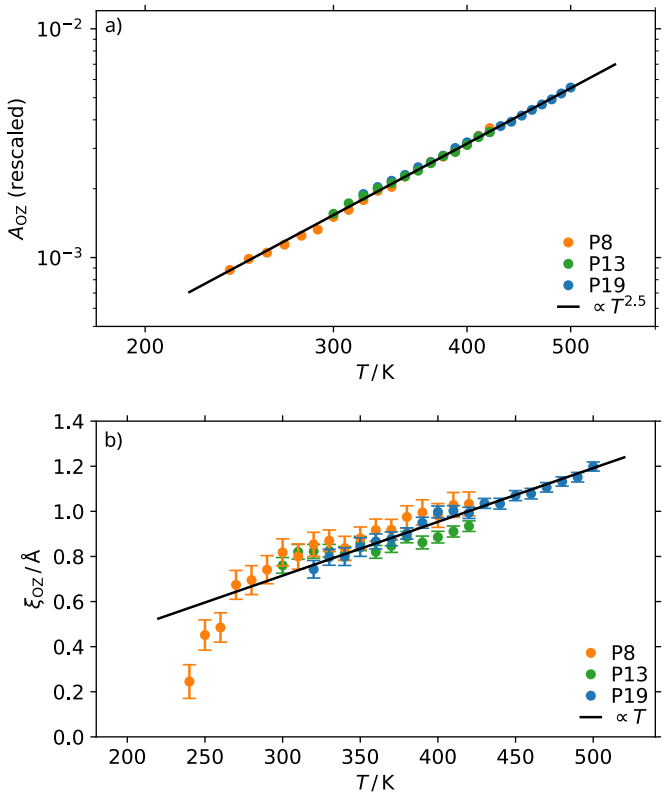

FIG. 2: a) Amplitude A_{OZ} of the Ornstein-Zernike function describing the plateau at low q values rescaled on to the data of P19. The black line is a fit of the P19 data by a power law $\propto T^{2.5}$. b) Characteristic length scale of the Ornstein-Zernike contribution ξ_{OZ}. The black line is a linear fit of the P19 data.

line). The data for the other samples were rescaled with a temperature independent prefactor to match the power law fit of the P19 data and as is seen in the figure, all data follow the P19 behavior to good approximation. We note that a similar plateau at low q increasing with temperature was observed by Patkowski and Fischer et al. for orthoterphenyl [2]. The observed increase of A_{OZ} with increasing temperature simply follows from eq. 2, since κ_T was shown to increase with temperature for linear and cyclic alkanes [3, 4] in a similar temperature range. Interestingly A_{OZ} does not show any change in temperature dependence between $n = 8$ and $n = 13$ in contrast to A_G indicating that the origin of this contribution is independent of the details of structure. Fig. 2 b) shows the temperature dependence of ξ_{OZ} for the 1-phenylalkanes. ξ_{OZ} shows an approximately linear temperature dependence for the 1-phenylalkanes, visualized

TABLE I: parameters of the small angle scattering models

parameter	Spheres in solution	Teubner-Strey
b: constant background	0.0020317	0.0020059
$\mathrm{SLD_a}$ / $(1 \times 10^{-6}\,\mathrm{Å}^{-2})$: scattering length density of component a	8	8
$\mathrm{SLD_b}$ / $(1 \times 10^{-6}\,\mathrm{Å}^{-2})$: scattering length density of component b	7.7644	7.7393
r / Å: sphere radius	8.4	
d / Å: domain size		20
v: volume fraction of component a	0.3	0.3
ξ / Å: coherence length		11.075
L: scale of Lorentzian	0.031711	0.031735
w_L / $\mathrm{Å}^{-1}$: HWHM of Lorentzian	0.22837	0.22879
$q_\mathrm{peak,L}$ / $\mathrm{Å}^{-1}$: position of Lorentzian	1.3848	1.3849

by the black line which is a linear fit to the data of P19. This increase in length scale with temperature is consistent with the interpretation of the contribution as arising from density fluctuations and hence the use of the Ornstein-Zernike equation. The length scale of the electron density fluctuations scales with the average distance between neighbouring molecules, which increases with increasing temperature due to the decreasing density. Furthermore, at a certain temperature, the correlation length values obtained for the different 1-phenylalkanes are similar, supporting this interpretation.

To conclude this supporting information we present a comparison of the chosen fit procedure to an alternative approach using standard models from small-angle scattering to substitute the prepeak Gaussian and the Ornstein-Zernike model. SasView (version 5.0.6) was used for this analysis. Two specific models were chosen for this comparison: spheres in solution and the Teubner-Strey model for microemulsions. These models do not extend into the high-q WAXS region of the main scattering peak and everything beyond the low q range is approximated by a constant background. However, since in our case the investigated q range includes the main scattering peak both models were combined with a Lorentzian peak function to account for the main scattering peak. The number of parameters is 9 for the Teubner-Strey approach, which is identical to the number of parameters of the fit procedure used in this work and 8 for the model of spheres in solution.

Fig. 3 shows a comparison of these models with the model used in this work for the example of P13 at 300 K. All three models are able to produce a peak like contribution below the main scattering peak. However, in case of the small angle scattering models assumptions on the exact nature of structures in the liquid are made before the process of fitting. Both models assume that the liquid consists of two components. Since the liquids studied here are one component liquids one would have to make the assumption that one component is represented by the alkyl chains and one by the phenyl rings. In case of spheres in solution regions of rings are represented by spheres with constant scattering length density ($\mathrm{SLD_a}$) and the alkyl chains are represented by a solvent with constant scattering length density ($\mathrm{SLD_b}$). The Teubner-Strey model assumes bicontinous domains of the two components [5]. Furthermore it proved impossible to arrive at a consistent description of the data without fixing certain parameters and the fits were also dependent on the starting values of the parameters. For this reason, the curves presented in Fig. 3 were obtained by fixing some parameters in a way that the obtained length scale matches that of the phenomenological fit model, which corresponds to $L = \frac{2\pi}{q_\mathrm{G,peak}} = 20\,\mathrm{Å}$ obtained from the position of the Gaussian. In both cases, the volume fraction v was set to 0.3 according to the approximate volume fraction of phenyl rings [6]. The periodicity d in the Teubner-Strey model was set to 20 Å and the radius of spheres r in the sphere model to $r = 8.4\,\mathrm{Å}$, which results in an average distance between sphere centers of 20 Å. Furthermore, fitting with free scattering length densities for both components resulted in unstable fits and the scattering length density of component a was therefore fixed to $8 \times 10^{-6}\,\mathrm{Å}^{-2}$, which is the value for toluene at room temperature. Due to the necessity of fixing parameters as well as the dependence on starting values for the small-angle scattering models the phenomenological approach was favored in this work.

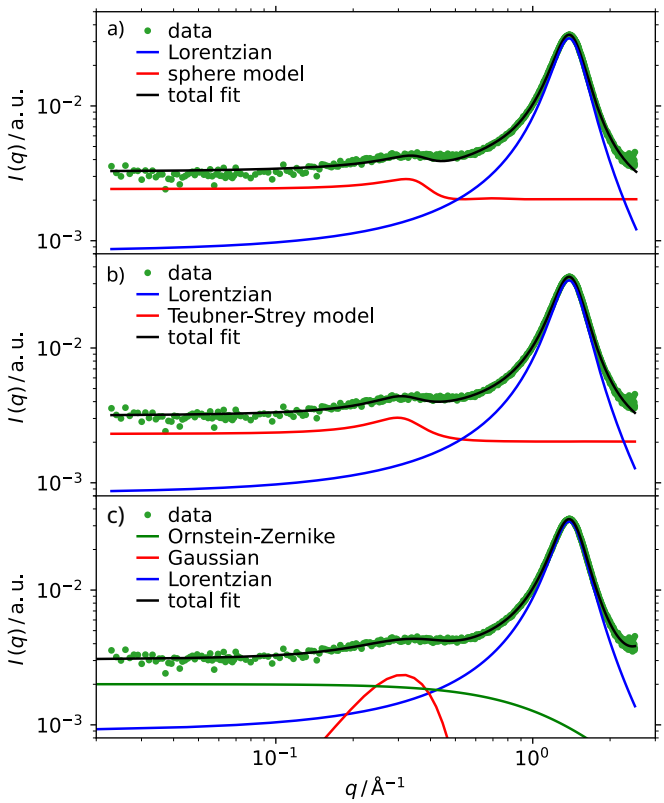

FIG. 3: Comparison of the phenomenological fit model used in this work and different small angle scattering models. From top to bottom: spheres in solution, Teubner-Strey model for micro emulsions and the model used in this work.

TABLE II: parameters obtained for P8 by fitting with eq. 1

T/K	$A_{OZ} \cdot 10^3$	ξ_{OZ} / Å	$A_G \cdot 10^4$	w_G / Å^{-1}	$q_{G,peak}$ / Å^{-1}	$A_{L1} \cdot 10^2$	w_{L1} / Å^{-1}	$q_{L1,peak}$ / Å^{-1}	$A_{L2} \cdot 10^3$
240	0.83(3)	0.25(8)	3.18(2)	0.189(8)	0.423(4)	1.97(1)	0.254(1)	1.414(1)	4.5(5)
250	0.93(3)	0.45(7)	2.74(2)	0.177(8)	0.425(5)	1.97(1)	0.256(1)	1.4128(1)	5.3(4)
260	0.99(3)	0.49(7)	2.79(2)	0.180(8)	0.433(5)	1.97(1)	0.258(1)	1.406(1)	5.4(3)
270	1.07(3)	0.67(7)	2.73(2)	0.180(8)	0.440(6)	1.99(1)	0.262(1)	1.400(1)	5.9(2)
280	1.17(3)	0.70(7)	2.88(2)	0.187(9)	0.445(6)	1.99(1)	0.266(1)	1.393(1)	5.6(2)
290	1.24(4)	0.74(7)	2.85(3)	0.189(10)	0.447(6)	2.00(1)	0.268(1)	1.388(1)	5.7(2)
300	1.41(3)	0.82(6)	2.64(2)	0.182(10)	0.455(7)	2.01(1)	0.271(1)	1.382(1)	5.5(2)
310	1.52(3)	0.80(6)	2.74(2)	0.179(9)	0.454(6)	2.02(1)	0.274(1)	1.376(1)	5.2(2)
320	1.67(3)	0.85(6)	2.67(2)	0.184(10)	0.456(7)	2.02(1)	0.276(1)	1.370(1)	5.3(2)
330	1.84(3)	0.87(5)	2.49(2)	0.173(9)	0.461(6)	2.01(1)	0.279(1)	1.364(1)	5.2(2)
340	1.91(3)	0.84(6)	2.79(3)	0.180(10)	0.456(7)	2.01(2)	0.281(1)	1.358(1)	4.9(2)
350	2.12(3)	0.88(5)	2.57(2)	0.176(10)	0.467(7)	2.02(2)	0.284(1)	1.353(1)	4.6(2)
360	2.27(3)	0.92(5)	2.59(3)	0.172(10)	0.461(7)	2.02(2)	0.286(1)	1.347(1)	4.7(2)
370	2.46(3)	0.92(5)	2.33(2)	0.170(10)	0.470(7)	2.01(2)	0.289(1)	1.342(1)	4.5(2)
380	2.59(4)	0.98(5)	2.76(3)	0.182(11)	0.466(7)	2.02(2)	0.292(2)	1.336(1)	4.5(2)
390	2.76(4)	1.00(6)	2.69(3)	0.190(13)	0.470(9)	2.02(2)	0.295(2)	1.330(1)	4.4(2)
400	2.92(5)	0.98(6)	2.84(4)	0.197(14)	0.457(9)	2.01(2)	0.297(2)	1.325(1)	4.1(2)
410	3.20(4)	1.03(6)	2.54(4)	0.197(15)	0.475(10)	2.02(2)	0.300(2)	1.320(1)	4.0(2)
420	3.45(4)	1.03(6)	2.36(4)	0.195(16)	0.471(11)	2.00(2)	0.301(2)	1.315(1)	3.7(2)

TABLE III: parameters obtained for P13 by fitting with eq. 1

T/K	$A_{OZ} \cdot 10^3$	ξ_{OZ} / Å	$A_G \cdot 10^4$	w_G / Å^{-1}	$q_{G,peak}$ / Å^{-1}	$A_{L1} \cdot 10^2$	w_{L1} / Å^{-1}	$q_{L1,peak}$ / Å^{-1}	$A_{L2} \cdot 10^3$
300	2.00(3)	0.76(4)	2.1(2)	0.124(7)	0.311(5)	2.38(1)	0.235(1)	1.386(1)	6.3(2)
310	2.23(4)	0.82(4)	1.8(2)	0.123(8)	0.308(5)	2.38(1)	0.238(1)	1.379(1)	6.0(2)
320	2.39(3)	0.82(4)	1.8(2)	0.124(8)	0.309(6)	2.37(1)	0.241(1)	1.373(1)	5.7(2)
330	2.58(3)	0.83(3)	1.7(2)	0.119(8)	0.312(6)	2.36(1)	0.243(1)	1.367(1)	5.5(2)
340	2.73(4)	0.81(4)	1.8(2)	0.123(9)	0.310(6)	2.36(1)	0.245(1)	1.361(1)	5.2(2)
350	2.92(4)	0.86(4)	1.7(2)	0.129(11)	0.305(7)	2.36(1)	0.249(1)	1.355(1)	5.1(2)
360	3.09(3)	0.82(3)	1.6(2)	0.117(9)	0.304(6)	2.34(1)	0.250(1)	1.349(1)	4.8(2)
370	3.33(4)	0.85(3)	1.5(2)	0.114(11)	0.301(7)	2.34(1)	0.253(1)	1.344(1)	4.7(2)
380	3.58(3)	0.89(3)	1.3(2)	0.109(10)	0.315(7)	2.34(1)	0.255(1)	1.338(1)	4.6(2)
390	3.73(4)	0.86(3)	1.5(2)	0.120(12)	0.302(8)	2.33(1)	0.258(1)	1.332(1)	4.1(2)
400	4.01(4)	0.89(3)	1.4(2)	0.109(11)	0.308(8)	2.32(1)	0.261(1)	1.327(1)	4.0(2)
410	4.33(4)	0.91(3)	1.1(2)	0.103(12)	0.301(9)	2.31(1)	0.262(1)	1.321(1)	3.8(2)
420	4.56(4)	0.93(3)	1.1(2)	0.104(12)	0.308(9)	2.31(1)	0.266(1)	1.316(1)	3.7(2)

TABLE IV: parameters obtained for P19 by fitting with eq. 1

T/K	$A_{OZ} \cdot 10^3$	ξ_{OZ} / Å	$A_G \cdot 10^4$	w_G / Å^{-1}	$q_{G,peak}$ / Å^{-1}	$A_{L1} \cdot 10^2$	w_{L1} / Å^{-1}	$q_{L1,peak}$ / Å^{-1}	$A_{L2} \cdot 10^3$
320	1.90(3)	0.74(4)	8.5(12)	0.094(9)	0.223(6)	2.04(1)(1)	0.225(1)	1.383(1)	6.3(2)
330	2.03(3)	0.80(4)	7.0(11)	0.085(10)	0.231(6)	2.05(1)	0.228(1)	1.378(1)	6.0(2)
340	2.17(4)	0.80(4)	7.1(13)	0.092(12)	0.228(7)	2.05(1)	0.231(1)	1.373(1)	6.0(2)
350	2.30(4)	0.84(5)	6.6(14)	0.090(14)	0.220(8)	2.06(1)	0.235(1)	1.367(1)	6.1(2)
360	2.48(3)	0.87(4)	6.3(12)	0.086(13)	0.229(8)	2.05(1)	0.237(1)	1.362(1)	5.9(2)
370	2.61(3)	0.88(4)	5.5(11)	0.077(12)	0.228(8)	2.06(1)	0.240(1)	1.357(1)	5.7(2)
380	2.79(3)	0.90(3)	4.7(9)	0.072(12)	0.242(8)	2.06(1)	0.243(1)	1.353(1)	5.4(2)
390	3.01(2)	0.95(3)	3.9(8)	0.066(13)	0.241(10)	2.06(1)	0.245(1)	1.347(1)	5.6(2)
400	3.19(3)	1.00(3)	3.9(8)	0.059(12)	0.235(10)	2.06(1)	0.249(1)	1.342(1)	5.5(2)
410	3.38(2)	1.00(3)	3.7(8)	0.056(11)	0.241(9)	2.06(1)	0.252(1)	1.337(1)	5.2(2)
420	3.53(3)	0.99(3)	3.8(9)	0.061(14)	0.218(10)	2.06(1)	0.255(1)	1.332(1)	5.0(2)
430	3.76(2)	1.04(3)	3.4(7)	0.052(11)	0.231(9)	2.06(1)	0.258(1)	1.327(1)	4.9(2)
440	3.92(3)	1.03(3)	4.4(10)	0.069(14)	0.223(11)	2.06(1)	0.260(1)	1.322(1)	4.7(2)
450	4.17(3)	1.07(3)	4.1(9)	0.064(14)	0.228(11)	2.06(1)	0.263(1)	1.317(1)	4.8(2)
460	4.42(3)	1.08(3)	2.7(10)	0.058(19)	0.217(15)	2.05(1)	0.266(1)	1.312(1)	4.6(2)
470	4.67(3)	1.11(3)	3.2(8)	0.048(12)	0.217(9)	2.05(1)	0.269(1)	1.307(1)	4.3(2)
480	4.91(3)	1.13(3)	2.6(9)	0.059(20)	0.221(15)	2.05(1)	0.272(1)	1.301(1)	4.3(2)
490	5.21(3)	1.15(3)	2.9(10)	0.055(17)	0.203(13)	2.04(1)	0.274(1)	1.296(1)	4.4(2)
500	5.54(3)	1.20(3)	2.1(9)	0.052(20)	0.211(15)	2.05(1)	0.278(1)	1.291(1)	4.0(2)

[1] J.-P. Hansen and I. R. McDonald, *Theory of simple liquids: with applications to soft matter*, Academic press, 2013.
[2] A. Patkowski, T. Thurn-Albrecht, E. Banachowicz, W. Steffen, P. Bösecke, T. Narayanan and E. W. Fischer, *Phys. Rev. E*, 2000, **61**, 6909.
[3] E. Aicart, G. Tardajos and M. D. Peña, *J. Chem. Therm.*, 1981, **13**, 783–788.
[4] T. Regueira, M.-L. Glykioti, E. H. Stenby and W. Yan, *J. Chem. Eng. Data*, 2017, **63**, 1072–1080.
[5] M. Teubner and R. Strey, *J. Chem. Phys.*, 1987, **87**, 3195–3200.
[6] Y. H. Zhao, M. H. Abraham and A. M. Zissimos, *J. Org. Chem.*, 2003, **68**, 7368–7373.